An Augmented Lagrangian-based Optimal Control: An Application towards an Electric Vehicle

Haris M. Khalid, *Member, IEEE*, Alya I. Al-Matrooshi, Fatma A. Al-Mulla, Shamma H. Al-Shamsi, Eman N. Al-Abboudi, Fatma I. Al-Marzooqi, Mariam A. Al Ansari, and Eman Y. M. Al-Ali

***Abstract*—Electric vehicles are a vital addition to the intelligent transportation systems. They bring features which could provide enhancements to decision making while improving on information and support systems. The critical nature of control is one of the main concerns for their advanced operations. In this work, the vehicle has been considered as a constrained system, where parameter optimization is required during the transition between different set-points of degree of freedom. Firstly, dynamics of the vehicle have been derived. Each vehicle dynamic has been monitored by a modeled sensor. Secondly, constrained optimization-based cost function has been set. This cost function is considered here to be the main building block for deriving augmented Lagrangian-based optimization to provide optimal control to the vehicle. Thirdly, co-states of the derived constraints are determined to maintain convergence. Numerical evaluations were made on a vehicle model. Results showed an ensured performance and accuracy of the proposed scheme.**

***Index Terms*—Augmented Lagrangian, autonomous vehicle, co-states, electric vehicle, estimation, optimal control, optimization.**

ACRONYMS AND ABBREVIATIONS OF MATHEMATICAL FORMULATIONS

AL	augmented Lagrangian
FWID	four-wheel independently driven
x	state variable
x_0	initial value of state variable
$\mathbf{R}$	subspace
r	size of the state vector
F	model matrix
$\mathcal{V}_x$	variable for longitudinal motion
α	transition matrix of longitudinal motion
$\mathcal{V}_y$	variable for lateral motion
β	transition matrix of lateral motion
Ω_z	variable for yaw motion
ϖ	transition matrix of yaw motion
G	noise transition matrix
w	random process noise
t	time instant
T	number of time-instants
y	observation output
m	number of simultaneous observations
H	observation matrix of state
ν	observation noise
C_a	aerodynamic drag
M	vehicle mass
$F_{xfl}, F_{xflr}, F_{xrl}, F_{xrr}$	tire longitudinal forces
$F_{yfl}, F_{yfr}, F_{yrl}, F_{yrr}$	tire lateral forces
σ	front steering angle
I_z	yaw inertia
l_s	longitudinal distance from side wheels
l_r	longitudinal distance from front wheels
l_f	longitudinal distance from rear wheels
J_E	energy-based cost function
ΔU	sequence of inputs
Ξ_1, Ξ_2, Ξ_3	Lagrange multipliers
$\Xi_{1,r}, \Xi_{2,r}, \Xi_{3,r}$	penalty coefficients

I. INTRODUCTION

The concept of renewable energy has shifted the trend from a fossil-fuel driven economy to a sustainable and green driven economy. This has also initiated a conceptual change in transportation sector, where zero-emission based electric vehicles (EVs) have been launched as a support system for a fossil-fuel free economy. The zero-emission based EVs do heavily rely on the battery packs as the main energy source. This is due to the use of electric motors, which are the primary source of propulsion in EVs. These EVs not only operate as a component of transportation, they also fill the gaps of energy short falls in electric power grids [1–5]. To be utilized as the only energy source, lithium-ion battery packs have hundreds of cells aligned in various structures, which are monitored to ensure accuracy and efficiency [6–8].

Since, the source of energy for the EVs is the non-liquid based lithium-ion batteries, the preferred vehicle architecture is four-wheel independently driven (FWID). This architecture is considered since it is run by four direct driven in-wheel motors. These in-wheel motors have such a structure so that: 1) emissions and fuel consumption can be reduced [9], and 2) all the wheels can be controlled independently [10]. The foremost reason of such an architecture is to have a fuel efficient propulsion system. Moreover, the independent access to each wheel has allowed to develop enhanced control strategies such as: 1) stability control system, 2) traction control system, 3) anti-lock braking system etc. However, due to the structural complexity of the concept with number of actuators, yaw moment and various types of torques (breaking torque, driving torque, output torque of an electric motor), failures and faults are the by-products. These failures may eventually jeopardize the vehicle motion control leading to instability or a vehicle crash. Several fault diagnosis and control strategies have been proposed in the literature [11–16]. Most of these papers are dealing with vehicle articles. [14–16] have dealt with independently driven architectures. The architectures have proposed solutions for component faults such as motor faults, bearing faults, current sensor fault, voltage sensor fault etc. However, there is a need where an optimal control of the vehicle could be achieved while keeping the vehicle stability limits.

In this paper, the FWID has been considered as a constrained optimization problem. The vehicle dynamics of longitudinal motion, lateral motion and yaw motion have been considered here. Since these dynamics have different set-points and degrees of freedom, this could provide degeneracy and dependency conditions, which would eventually result the vehicle motion to destabilize. The proposed solution considered Augmented Lagrangian to achieve an optimal control of the vehicle while keeping the vehicle in stability limits. To ensure the stability of vehicle, co-states of the vehicle dynamics are determined to maintain convergence.

The write-up of this paper is made as follows: The proposed constrained optimization structure is formulated in Section II. Implementation and evaluation of the scheme is made in Sec-

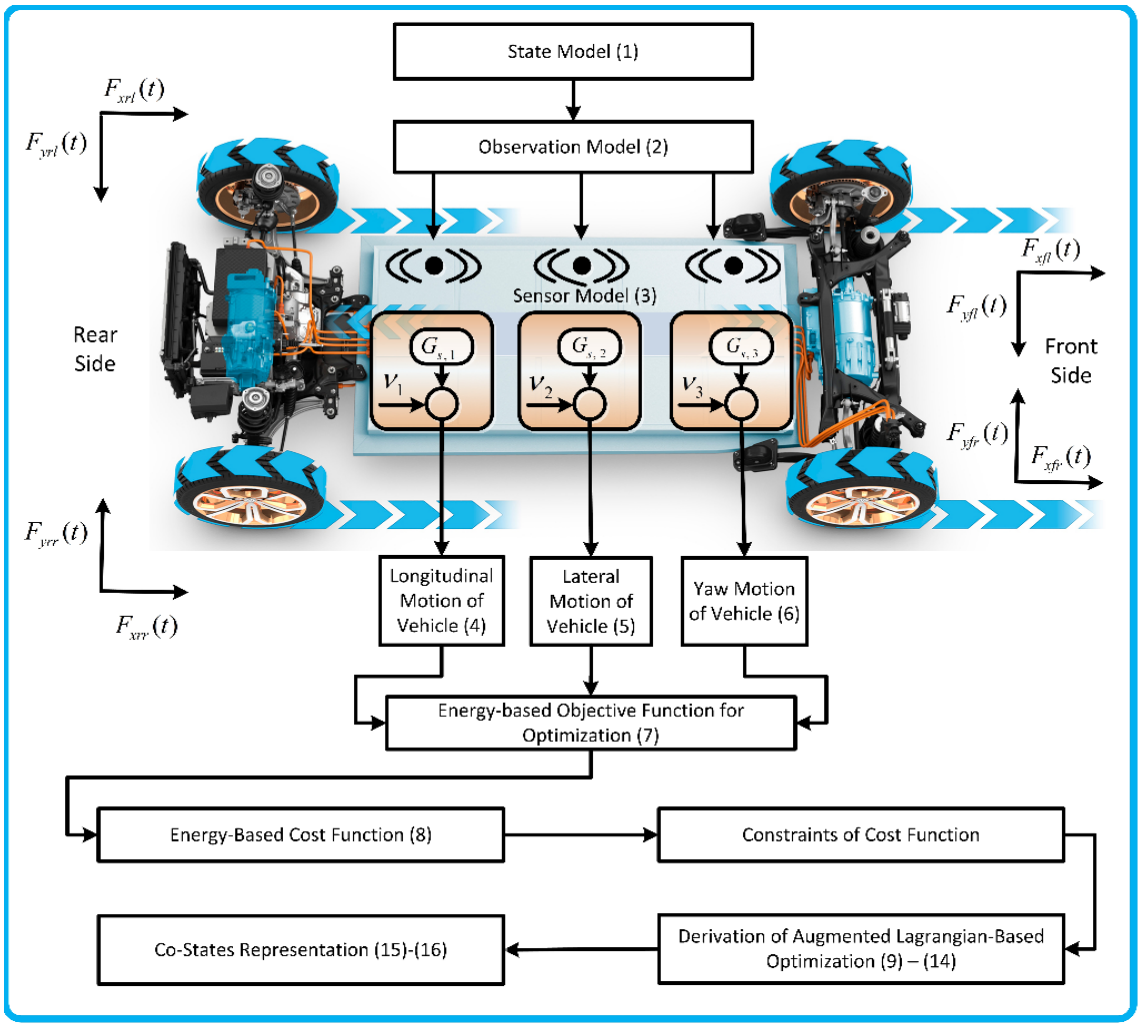

Fig. 1. Proposed framework of constrained optimization

tion III. Conclusions are made in Section IV.

II. Problem Formulation

The problem is formulated based on the constrained optimization structure as shown in Fig. 1.

A. Constrained Optimization Structure

The structure is explained in Fig. 1. It elaborates the steps involved in the framework. 1) A state model is expressed here, 2) An observation model is built on the state model, dynamics of electric ground vehicle are derived in (3), longitudinal motion, lateral motion, and yaw motion of the vehicle in (4)-(6) respectively. An energy-based objective function for AL-based optimization is expressed in (7). This is followed by building a cost function in (8). Constraints of the cost function are then defined. Derivation of Augmented Lagrangian with the cost function is made in (9)-(14), and finally, co-state representation is made in (15)-(16).

1) State Model: Consider a discrete-time dynamical n-*th* order system of a four-wheeled independently driven (FWID) electric ground vehicle [9]. It has been assumed that the vehicle has only three degrees of freedom for motion, which are 1) longitudinal motion, 2) lateral motion, and 3) yaw motion. The state representation of such a model can be expressed as:

$$x(t+1) = F(t)x(t) + \alpha(t)\mathcal{V}_x(t) + \beta(t)\mathcal{V}_y(t) + \varpi(t)\Omega_z(t) + G(t)w(t) \quad (1)$$

where $x_0(t) \in \mathbf{R}^{n\times 1}$ is the initial condition of the state of vehicle at time-instant t. $F(t) \in \mathbf{R}^{n\times n}$ is a model matrix of the state response, $\mathcal{V}_x(t) \in \mathbf{R}^{n\times 1}$ is the variable for longitudinal motion, and $\alpha(t) \in \mathbf{R}^{n\times n}$ is the transition matrix of longitudinal motion. $\mathcal{V}_y(t) \in \mathbf{R}^{n\times 1}$ is the variable for lateral motion, and $\beta(t) \in \mathbf{R}^{n\times n}$ is the transition matrix of lateral motion. $\Omega_z(t) \in \mathbf{R}^{n\times 1}$ is the variable for yaw motion, and $\varpi(t) \in \mathbf{R}^{n\times n}$ is the transition matrix of yaw motion. $G(t) \in \mathbf{R}^{n\times n}$ is the noise transition matrix, which can be defined as a probability vector whose elements are non-negative real numbers and sum to 1. $w(t) \in \mathbf{R}^{n\times 1}$ is the random process noise, t is the time instant, and T refers to the number of time instants.

2) Observation Model: Let the electric vehicle described in

(1) be observed at time-instant t as:

$$y(t) = H(t)x(t) + \nu(t) \tag{2}$$

where $y(t) \in \mathbf{R}^{m\times 1}$ is the observation output of state of vehicle, m is the number of simultaneous observations for estimation made at time instant t, $H(t) \in \mathbf{R}^{m\times n}$ is the observation matrix of state, and $\nu(t) \in \mathbf{R}^{m\times 1}$ is the observation noise.

Once the observation model is extracted from the dynamics of electric ground vehicle, the sensor model is defined for each degree of freedom.

3) Sensor Model: A sensor is modeled by a gain and an additive noise, as given below:

$$\Upsilon_{s,i}(t) = G_{si}\Upsilon^0_{s,i} + \nu_{s,i} \tag{3}$$

where $\Upsilon_{s,i}$, $\Upsilon^0_{s,i}$, and $\nu_{s,i}$ are the measured sensor output, true or fault-free output and additive sensor noise, respectively for an i-th sensor. Here i is equal to 1, 2 or 3 for the longitudinal, lateral and yaw motion respectively. Here the gain G_{si} is such that $0 \leq G_{s,i} \leq 1$, with the degree of the fault ranging from no fault at all for $G_{s,i} = 1$ to a complete failure for $G_{si} = 0$.

Once the sensor model is defined, the motion equations for each degree of freedom are expressed.

4) Longitudinal motion of vehicle: Vehicle equations of motion can be expressed in detail in [16]. The longitudinal motion $\mathcal{V}_x(t)$ can be represented as:

$$\begin{aligned}\hat{\mathcal{V}}_x(t) = \mathcal{V}_y(t)\Omega_z(t) - \frac{C_a(t)}{M(t)}\mathcal{V}^2_x(t) + \frac{1}{M(t)}\Big[F_{xfl}(t) \\ + F_{xfr}(t)\cos\sigma - \Big(F_{yfl}(t) + F_{yfr}(t)\Big)\sin\sigma + F_{xrl}(t) \\ + F_{xrr}(t)\Big]\end{aligned} \tag{4}$$

where $C_a(t)$ is the aerodynamic drag, $M(t)$ is the mass of vehicle. $F_{xfl}(t)$, $F_{xflr}(t)$, $F_{xrl}(t)$, and $F_{xrr}(t)$ are the tire longitudinal forces. σ is the front steering angle.

5) lateral motion of vehicle: The lateral motion $V_y(t)$ is represented as:

$$\begin{aligned}\hat{\mathcal{V}}_y(t) = -\mathcal{V}_x(t)\Omega_z(t) + \frac{1}{M(t)}\Big[F_{yfl}(t) + F_{yfr}(t)\cos\sigma \\ - \Big(F_{xfl}(t) + F_{xfr}(t)\Big)\sin\sigma + F_{yrl}(t) + F_{yyr}(t)\Big]\end{aligned} \tag{5}$$

where $F_{yfl}(t)$, $F_{yfr}(t)$, $F_{yrl}(t)$, and $F_{yrr}(t)$ are the tire lateral forces.

6) Yaw motion of vehicle: The yaw motion is shown as:

$$\begin{aligned}\hat{\Omega}_z(t) = \frac{1}{I_z(t)}\Big[\Big(F_{yfl}(t)\sin\sigma - F_{xfl}(t)\cos\sigma - F_{xrl}(t) \\ + F_{xrr}(t) + F_{xfr}(t)\cos\sigma - F_{yfr}(t)\sin\sigma\Big)l_s(t) \\ - \Big(F_{yfr}(t) + F_{yrr}(t)\Big)l_r(t) + \Big((F_{yfr}(t) + F_{xfl}(t)) \\ \cos\sigma + (F_{xfr}(t) + F_{xfl}(t))\sin\sigma\Big)l_f(t)\Big]\end{aligned} \tag{6}$$

where $I_z(t)$ is the yaw inertia. $l_s(t)$, $l_r(t)$ and $l_f(t)$ are the longitudinal distances from the center-of-gravity of vehicle to side, front and rear wheels respectively.

To control the degrees of motion, the computation of individual dynamics is required. This is handled by developing a constrained optimization model for the system, which could optimize each motion variable by considering it as a subproblem. This would contribute towards the original objective function of controlling the electric ground vehicle. In order to achieve that, an augmented Lagrangian-based solution is proposed here.

7) Energy-based Objective Function for Augmented Lagrangian-Based Optimization: The objective of optimal control is to bring the estimated $\hat{\mathcal{V}}_x(t)$, $\hat{\mathcal{V}}_y(t)$, and $\hat{\Omega}_z(t)$ as close as possible to the reference (set-point) profiles. The energy-based objective function $f(E)$ is defined as:

$$\begin{aligned}f(E) = \Big(\mathcal{V}_x(t) - \hat{\mathcal{V}}_x(t)\Big)'\Big(\mathcal{V}_x(t) - \hat{\mathcal{V}}_x(t)\Big) + \Big(\mathcal{V}_y(t) - \hat{\mathcal{V}}_y(t)\Big)' \\ \Big(\mathcal{V}_y(t) - \hat{\mathcal{V}}_y(t)\Big) + \Big(\Omega_z(t) - \hat{\Omega}_z(t)\Big)'\Big(\Omega_z(t) - \hat{\Omega}_z(t)\Big) \\ + \Delta U(T)'F(T)\end{aligned} \tag{7}$$

where $\Delta U(T)$ is the variable representing sequence of inputs from the current observed states at time-instant t, such that $\Delta U(T) = [\Delta U(t), ...\Delta U(t+T)]$. A symbol $'$ over a variable represents the transpose operator. $F(T)$ is a compatible vector.

This would now define the cost function for minimization.

8) Energy-Based Cost Function: The energy-based cost function can be represented as:

$$J_E = \min \Delta U(T) = \frac{1}{2}\mathcal{V}^2_x(t) + \frac{1}{2}\mathcal{V}^2_y(t) + \frac{1}{2}\Omega^2_z(t) \tag{8}$$

9) Constraints of Cost Function: Constraints for this cost-function are defined. The first constraint represents the longitudinal motion as $\mathcal{V}_x(t+1) = \mathcal{V}_x(t) + \Big[\mathcal{V}_y(t)\Omega_z(t) - \frac{C_a(t)}{M(t)}\mathcal{V}^2_x(t) + \frac{1}{M(t)}[F_{xfl}(t) + F_{xfr}(t)\cos\sigma - \Big(F_{yfl}(t) + F_{yfr}(t)\Big)\sin\sigma + F_{xrl}(t) + F_{xrr}(t)]\Big] \times \tau_s$. The second constraint is about the lateral motion. It is represented as $\mathcal{V}_y(t+1) = \mathcal{V}_y(t) + \Big[-\mathcal{V}_x(t)\Omega_z(t) + \frac{1}{M(t)}[F_{yfl}(t) + F_{yfr}(t)\cos\sigma - \Big(F_{xfl}(t) + F_{xfr}(t)\Big)\sin\sigma + F_{yrl}(t) + F_{yyr}(t)]\Big] \times \tau_s$. The third constraint is on yaw motion as $\Omega_z(t+1) = \Omega_z(t) + \Big[\frac{1}{I_z(t)}[\Big(F_{yfl}(t)\sin\sigma - F_{xfl}(t)\cos\sigma - F_{xrl}(t) + F_{xrr}(t) + F_{xfr}(t)\cos\sigma - F_{yfr}(t)\sin\sigma\Big)l_s(t) - \Big(F_{yfr}(t) + F_{yrr}(t)\Big)l_r(t) + \Big((F_{yfr}(t) + F_{xfl}(t))\cos\sigma + (F_{xfr}(t) + F_{xfl}(t))\sin\sigma\Big)l_f(t)]\Big] \times \tau_s$.

10) Derivation of cost function with AL: The augmented Lagrangian-based optimization can be derived here. This will be achieved while considering J_E as the main function, $\Xi(t)$ as Lagrange multiplier, and $\Xi_r(t)$ as augmented Lagrange multiplier, such that $\Xi(t)$, $\Xi_r(t) \geq 0$ as:

$$\begin{aligned}J_E = \frac{1}{2}\mathcal{V}^2_x(t) + \frac{1}{2}\mathcal{V}^2_y(t) + \frac{1}{2}\Omega^2_z(t) - \Xi_1(t) \times \Big[\mathcal{V}_x(t+1) \\ - \mathcal{V}_x(t) - \Big[\mathcal{V}_y(t)\Omega_z(t) - \frac{C_a(t)}{M(t)}\mathcal{V}^2_x(t) + \frac{1}{M(t)}[F_{xfl}(t) \\ + F_{xfr}(t)\cos\sigma - \Big(F_{yfl}(t) + F_{yfr}(t)\Big)\sin\sigma + F_{xrl}(t) \\ + F_{xrr}(t)]\Big] \times \tau_s\Big] - \Xi_{1,r}(t) \times \Big[\mathcal{V}_x(t+1) - \mathcal{V}_x(t) \\ - \Big[\mathcal{V}_y(t)\Omega_z(t) - \frac{C_a(t)}{M(t)}\mathcal{V}^2_x(t) + \frac{1}{M(t)}[F_{xfl}(t) + F_{xfr}(t)\end{aligned}$$

$$\cos\sigma - \Big(F_{yfl}(t) + F_{yfr}(t)\Big)\sin\sigma + F_{xrl}(t) + F_{xrr}(t)\Big] \times \tau_s\Big]^2 - \Xi_2(t) \times \Big[\mathcal{V}_y(t+1) - \mathcal{V}_y(t) - \Big[\mathcal{V}_x(t)\Omega_z(t) + \frac{1}{M(t)}[F_{yfl}(t) + F_{yfr}(t)\cos\sigma - (F_{xfl}(t) + F_{xfr}(t)) \sin\sigma + F_{yrl}(t) + F_{yyr}(t)]\Big] \times \tau_s\Big] - \Xi_{2,r}(t) \times \Big[\mathcal{V}_y(t+1) - \mathcal{V}_y(t) - \Big[\mathcal{V}_x(t)\Omega_z(t) + \frac{1}{M(t)}[F_{yfl}(t) + F_{yfr}(t)\cos\sigma - (F_{xfl}(t) + F_{xfr}(t))\sin\sigma + F_{yrl}(t) + F_{yyr}(t)]\Big] \times \tau_s\Big]^2 - \Xi_3(t) \times \Big[\Omega_z(t+1) - \Omega_z(t) - \Big(\frac{1}{I_z(t)}\Big(F_{yfl}(t)\sin\sigma - F_{xfl}(t)\cos\sigma - F_{xrl}(t) + F_{xrr}(t) + F_{xfr}(t)\cos\sigma - F_{yfr}(t)\sin\sigma\Big)l_s(t) - \Big(F_{yfr}(t) + F_{yrr}(t)\Big)l_r(t) + \Big((F_{yfr}(t) + F_{xfl}(t))\cos\sigma + (F_{xfr}(t) + F_{xfl}(t))\sin\sigma\Big) l_f(t)] \times \tau_s\Big] - \Xi_{3,r}(t) \times \Big[\Omega_z(t+1) - \Omega_z(t) - \Big(\frac{1}{I_z(t)} \Big(F_{yfl}(t)\sin\sigma - F_{xfl}(t)\cos\sigma - F_{xrl}(t) + F_{xrr}(t) + F_{xfr}(t)\cos\sigma - F_{yfr}(t)\sin\sigma\Big)l_s(t) - \Big(F_{yfr}(t) + F_{yrr}(t)\Big)l_r(t) + \Big((F_{yfr}(t) + F_{xfl}(t))\cos\sigma + (F_{xfr}(t) + F_{xfl}(t))\sin\sigma\Big)l_f(t)] \times \tau_s\Big]^2 \quad (9)$$

where $\Xi_1(t)$, $\Xi_2(t)$ and $\Xi_3(t)$ are the Lagrange multipliers. $\Xi_{1,r}(t)$, $\Xi_{2,r}(t)$ and $\Xi_{3,r}(t)$ are the penalty coefficients. Assuming (9) admits a 1) feasible solution, and 2) each dynamics involved when $J_E \in \zeta$ is solved, where ζ belongs to subspace $\mathbf{R}^n$.

Minimizing J_E with respect to $\mathcal{V}_x(t)$ gives:

$$\frac{\delta J_E}{\delta \mathcal{V}_x(t)} = \mathcal{V}_x(t) + \Xi_1(t) \times \tau_s - 2\Xi_1(t)\frac{C_a(t)}{M(t)}\mathcal{V}_x^2(t) \times \tau_s + 2\Xi_{1,r}(t)\mathcal{V}_x(t) \times \tau_s - 2\Xi_{1,r}(t)\frac{C_a(t)}{M(t)}\mathcal{V}_x^2(t)2\mathcal{V}_x(t) \times \tau_s - \Xi_2(t)\Omega_z(t) \times \tau_s - 2\Xi_{2,r}(t)\mathcal{V}_x(t)\Omega_z(t) \times \tau_s \quad (10)$$

Minimizing J_E with respect to $\mathcal{V}_y(t)$ gives:

$$\frac{\delta J_E}{\delta \mathcal{V}_y(t)} = \mathcal{V}_y(t) + \Xi_1(t)\Omega_z(t)\tau_s + \Xi_{1,r}(t)2\mathcal{V}_y(t)\Omega_z(t)\tau_s 2\Omega_z(t)\tau_s + \Xi_2(t)\tau_s + \Xi_{2,r}(t)2\mathcal{V}_y(t)\tau_s \quad (11)$$

Minimizing J_E with respect to $\Omega_z(t)$ gives:

$$\frac{\delta J_E}{\delta \Omega_z(t)} = \Omega_z(t) + \Xi_1(t)\mathcal{V}_y(t)\tau_s - 2\Xi_{2,r}(t)\mathcal{V}_y(t)\Omega_z(t)\tau_s \mathcal{V}_y(t)\tau_s - \Xi_2(t)\mathcal{V}_x(t)\tau_s - 2\Xi_{2,r}(t)\mathcal{V}_x(t)\Omega_z(t)\tau_s \mathcal{V}_x(t)\tau_s - \Xi_3(t)\tau_s - 2\Xi_{3,r}(t)\Omega_z(t)\tau_s^2 \quad (12)$$

Considering the Lagrange multipliers, minimizing J_E with respect to $\mathcal{V}_x(t)$ gives:

$$0 = \mathcal{V}_x(t) + \Xi_1(t) \times \tau_s - 2\Xi_1(t)\frac{C_a(t)}{M(t)}\mathcal{V}_x^2(t)\mathcal{V}_x(t)\tau_s - \Xi_2(t)\Omega_z(t) \times \tau_s \quad (13)$$

Considering the Lagrange multipliers, minimizing J_E with respect to $\mathcal{V}_y(t)$ gives:

$$0 = \mathcal{V}_y(t) + \Xi_1(t)\Omega_z(t) \times \tau_s + \Xi_2(t) \times \tau_s \quad (14)$$

Similarly for $\Omega_z(t)$ gives:

$$0 = \Omega_z(t) + \Xi_1(t)\mathcal{V}_y(t) \times \tau_s - \Xi_2(t)\mathcal{V}_x(t) \times \tau_s - \Xi_3(t) \times \tau_s \quad (15)$$

11) Co-States Representation: The co-states $\Xi_k(t)$ are determined by backward integration of the adjunct state equation yielding:

$$\begin{bmatrix}\Xi_1\\ \Xi_2\\ \Xi_3\end{bmatrix}_{t-1} = -2h(t)\frac{\delta E_d}{\delta x(t)} - F(t)^{'}\lambda(t) -h(t)[\sum_{i=1}^{N}\nabla_{x(t)}\psi_{\mu s}(\sigma(t)^i, s_i^{dl}(x(t)))] -h(t)[\sum_{j=1}^{N}\nabla_{x(t)}\psi_{\mu g}(\varrho(t)^j, g_j^D(x(t),\nu(t),h(t)))] \quad (16)$$

where,

$$x(t+1) = f_{d_z}^D(x(t),\tau(t),h(t)), t = 0,.....,N-1$$
$$g_j^D(x(t),\nu(t),h(t)) \leq 0,\ j \in \{1,2,.....j\}$$
$$F_d^{'} = I_d$$
$$E_d = \mathcal{V}_x(t), \mathcal{V}_y(t), \Omega_z(t) \quad (17)$$

III. Numerical Results

The numerical results have been generated here. The derived vehicle dynamics (4)-(6), energy-based objective and cost function (7)-(8), derivation of cost-function with AL (9)-(14), minimization with respect to states and co-states (15)-(16) are considered for the simulation. The parameters considered are as follows: mass of vehicle M is $1410\ kg$, yaw moment of inertia Ω_z is $1800\ kgm^2$, longitudinal distances from center-of-gravity to side l_s, front l_f and rear l_r are: $1000\ m$, $1100\ m$ and $1500\ m$ respectively. It can be seen in Fig. 2 that initially the lateral motion and yaw motion suffered to converge due to their different axis of freedom. However, all the three motions were optimally controlled while achieving a steady-state value. This is due to the property of the Augmented Lagrangian-based optimization and its co-states which ensured convergence of all degrees of motion.

IV. Conclusions

The optimal control of an FWID-based electric vehicle is analyzed here. Various degrees of freedom have been considered for the control design. The proposed scheme was able to adequately provide an optimal control to the vehicle. This was achieved by optimizing the degrees of freedom on the same scale and deriving a subproblem-based minimization for all the constraints. Future work would involve to develop a robust control which could tackle all the uncertainties and perturbations of vehicle dynamics.

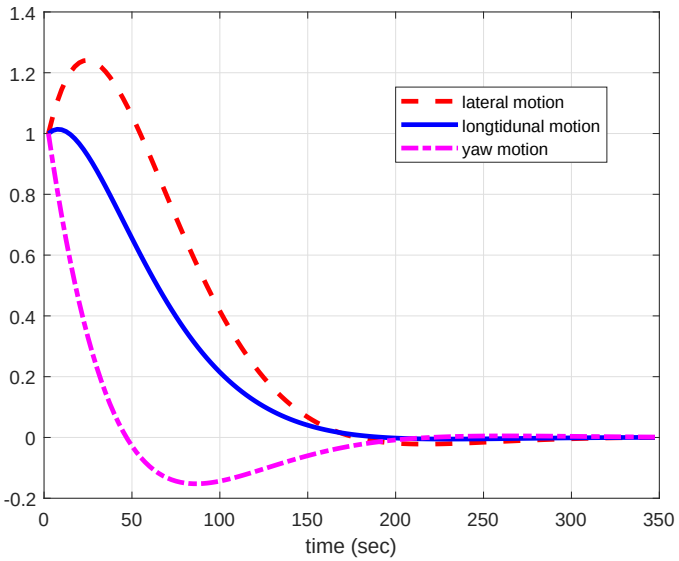

Fig. 2. Optimal control of degrees of motion using augmented Lagrangian

REFERENCES

[1] S. Morse and K. Glitman, "Electric vehicles as grid resources in ISO-NE and Vermont," *https://www.veic.org/documents/default-source/resources/reports/evt-rd-electric-vehicles-grid-resource-final-report.pdf*, *Technical Report*, pp. 1–44, May 2014.

[2] M. Aziz, T. Oda, T. Mitani, Y. Watanabe and T. Kashiwagi, "Utilization of electric vehicles and their used batteries for peak-load shifting," *Energies*, vol. 8, no. 5, pp. 3720-3738, Apr. 2015.

[3] H. Xing, Z. Lin, M. Fu, "A new decentralized algorithm for optimal load shifting via electric vehicles," *Proc. 36th Chinese Control Conference*, Dalian, China, pp. 10708–10713, July 26-28, 2017.

[4] G. Wenzel, M. Negrete-Pincetic, D. E. Olivares, J. MacDonald, and D. S. Callaway, "Real-time charging strategies for an electric vehicle aggregator to provide ancillary services," *IEEE Trans. Smart Grid*, pp. 1–11, Article in Press, 2018.

[5] X. Wang, and Q. Liang, "Energy management strategy for Plug-In hybrid electric vehicles via bidirectional Vehicle-to-Grid," *IEEE Systems J.*, vol. 11, no. 3, pp. 1789-1798, Sep. 2017.

[6] H. M. Khalid, Q. Ahmed and J. C.-H. Peng, "Health monitoring of Li-ion battery systems: A median expectation-based diagnosis approach (MEDA)", *IEEE Transactions on Transportation Electrification*, vol. 1, no. 1, pp. 94–195, June 2015.

[7] H. M. Khalid, Q. Ahmed, J. C.-H. Peng and G. Rizzoni, "Current-split estimation in Li-ion battery pack: An enhanced weighted recursive filter method", *IEEE Transactions on Transportation Electrification*, vol. 1, no. 4, pp. 402–412, December 2015.

[8] H. M. Khalid, Q. Ahmed, J. C.-H. Peng and G. Rizzoni, "Pack-level current-split estimation for health monitoring in Li-ion batteries", *American Control Conference (ACC)*, Boston, MA, USA, 6-8 July, 2016.

[9] C. C. Chan, "The state of the art of electric and hybrid vehicles," *Proceedings of the IEEE*, pp. 247–275, vol. 90, no. 2, Feb. 2002.

[10] Y. Hori, "Future vehicle driven by electricity and control-Research on four-wheel-motored "UOT electric march II"," *IEEE Transactions on Industrial Electronics*, pp. 954–962, vol. 51, no. 5, Oct. 2004.

[11] R. Wang and J Wang, "In-wheel motor fault diagnosis for electric ground vehicles," *Proceedings of the 2010 ASME Dynamic Systems and Control Conference*, paper No. DSCC2010-4050, pp. 133–140, 2010.

[12] R. Wang and J. Wang, "Fault-tolerant control of electric ground vehicles with independently-actuated wheels," *Proceedings of the 2010 ASME Dynamic Systems and Control Conference*, vol. 134, no. 2, pp. 021014–021014-10, 2012.

[13] Jayabalan, R., and Fahimi, B. "Monitoring and fault diagnosis of multi-converter systems in hybrid electric vehicles," *IEEE Transactions on Vehicular Technology*, vol. 55, no. 5, pp. 1475–1484, 2006.

[14] H. Yang, V. Cocquempot, and B. Jiang, "Optimal fault-tolerant path-tracking control for 4WS4WD electric vehicles," *IEEE Transactions on Intelligent Transportation Systems*, vol. 11, no. 1, pp 237–243, 2010.

[15] H. Yang, V. Cocquempot, and B. Jiang, "Hybrid fault tolerant tracking control design for electric vehicles," *16th Mediterranean Conference on Control and Automation Congress Centre*, Ajaccio, France, June 25-27, 2008.

[16] R. Wang, and J. Wang, "Fault tolerant control with active fault diagnosis for four-wheel independently-driven electric ground vehicles," *American Control Conference*, pp. 3954–3959, Jun. 29–Jul. 01, 2011, USA.